NEWS & VIEWS

EARTH SCIENCE

River incision revisited

A data–set compilation suggests that measurements of river erosion into rock depend on the observation timescale, casting doubt on whether terraces and other incised landforms faithfully record changes in climate and tectonics. SEE LETTER P.391

ROMAN A. DIBIASE

The pattern and ages of relict landforms, such as terraces, that are incised by rivers provide the best record of changes in Earth's surface elevation over millennial to million-year timescales. As a result, much work has been devoted to determining the age of bedrock landforms[1] and sediment deposited on terraces[2] and in caves[3], to constrain the magnitude and timing of river incision. On page 391 of this issue, Finnegan *et al.*[4] challenge the perception that the ages of relict landforms along incised bedrock rivers (Fig. 1) retain a signature of climatic and tectonic forcing. Instead, the authors argue that the intermittent nature of bedrock river incision means that attempts to measure long-term incision rates are inherently biased by the timescale over which they are averaged.

Bedrock rivers set the pace of landscape evolution and form an important connection between Earth's tectonic and climatic systems. As mountain ranges are uplifted, increases in topographic relief cause rivers to incise bedrock towards a balance between erosion and uplift. Furthermore, the ability of rivers to incise rock and transport sediment is controlled by the size and frequency of floods. Such floods are sensitive to changes in climate that may in turn be driven by tectonic processes. In recent decades, provocative hypotheses[5] regarding the potential coupling of climate, tectonics and erosion have impelled the need for a quantitative understanding of the mechanics of river incision[6].

The idea of a link between the rates of change in surface elevation and the measurement timescale is well known in stratigraphy; this bias is known as the Sadler effect, after its discovery[7] by Earth scientist Peter Sadler. In the sedimentary record, depositional history is not continuous, but is broken by gaps of non-deposition or erosion, owing to the dynamics of sedimentary processes. As a

Figure 1 | A flight of river terraces in the Tian Shan foreland, China. Finnegan *et al.*[4] argue that river incision rates into bedrock, determined from dated landforms such as these, are biased by the timescale over which they are measured.

result, measurements of deposition rates over timescales shorter than the longest gap will overestimate long-term averages in a predictable manner[8]. Might a similar bias be present in net erosional landscapes?

Finnegan *et al.* approached this problem by compiling a global data set of incision records from dated terraces, caves and lava flows. They show that, in general, incision rates decrease with increasing measurement interval. The authors combed published studies for field sites that have multiple levels of dated incised landforms spanning a wide range in age, and

analysed records from diverse tectonic settings — including the rapidly uplifting middle gorge of the Indus River in the Himalayas and rivers draining the tectonically quiescent Appalachian Mountains in the eastern United States. They found that, in 11 of 14 locations, apparent incision rates increase towards the present day. This relationship holds across four orders of magnitude in landform age, from thousands to tens of millions of years, and is independent of tectonic setting or landform type.

The researchers reasoned that the observed scaling relationship is due to the intermittency of river incision, and they employed a random-walk model to show this effect. In the model, as the time window of observation increases, so does the likelihood of experiencing a long period without erosion, and an inverse power law scaling between the inferred incision rate and measurement interval emerges. Finnegan *et al.* propose that the hiatuses in river incision occur when sediment covers and protects the river bed from erosion, and are analogous to gaps in the sedimentary record. This implies that erosional as well as depositional landscapes are subject to an observational bias when deriving rates that average over different time spans.

The similarity in scaling behaviour for sites from a wide range of tectonic settings hints at the existence of a common driver for the perceived acceleration of incision rates, but there are a few factors that complicate this interpretation. First, abandoned flights of terraces and deep valleys that preserve incision markers are the precise landforms expected for landscapes undergoing an actual increase in erosion as a result of changes in climate or tectonics[9]. Further independent information from these landscapes is needed to provide constraints on the plausibility of the steady-state erosion implicitly assumed by Finnegan and colleagues.

Second, although there is little argument that river incision occurs only intermittently,

and that deposition in response to landslides can protect river beds from eroding over millennial timescales[10], it is unclear what physical processes drive hiatuses in incision over timescales of 1 million to 10 million years. Such long timescales span multiple glacial–interglacial climate cycles, and may also reflect a connection to deep Earth processes. Perhaps the most intriguing implication of Finnegan and co-workers' study is the idea that long-term rates of landscape lowering may be more sensitive to the frequency and magnitude of depositional events than to the mechanics of river incision into bedrock.

If the authors' findings hold true, a natural question arises: can changes in the pace of landscape evolution be deciphered from net erosional landscapes? Work on depositional landscapes shows that the preservation bias in one-dimensional stratigraphy disappears when the spatial distribution of both preserved sediments and hiatuses within a basin are taken into account[11–13]. By incorporating a similar spatial averaging in erosional landscapes[12,13], or by accounting for changes in hillslope lowering over time using different chronometers[14], it may be possible to overcome some of these biases.

Finally, to understand the influence of tectonics, land use or climate change on erosion rates, we need a robust way to compare rates measured over different time intervals. Although this is a challenging task, characterizing the degree to which these rates are unsteady, by studying the processes that control erosion and deposition, is essential for interpreting rates measured over different periods of Earth's history and for predicting future change. ∎

Roman A. DiBiase *is in the Division of Geological and Planetary Sciences, California Institute of Technology, Pasadena, California 91125, USA.*
e-mail: rdibiase@caltech.edu

1. Leland, J., Reid, M. R., Burbank, D. W., Finkel, R. & Caffee, M. *Earth Planet. Sci. Lett.* **154,** 93–107 (1998).
2. Anderson, R. S., Repka, J. L. & Dick, G. S. *Geology* **24,** 47–51 (1996).
3. Granger, D. E., Kirchner, J. W. & Finkel, R. C. *Geology* **25,** 107–110 (1997).
4. Finnegan, N. J., Schumer, R. & Finnegan, S. *Nature* **505,** 391–394 (2014).
5. Raymo, M. E. & Ruddiman, W. F. *Nature* **359,** 117–122 (1992).
6. Whipple, K. X. *Nature Geosci.* **2,** 97–104 (2009).
7. Sadler, P. M. *J. Geol.* **89,** 569–584 (1981).
8. Schumer, R. & Jerolmack, D. J. *J. Geophys. Res.* **114,** F00A06 (2009).
9. Crosby, B. T. & Whipple, K. X. *Geomorphology* **82,** 16–38 (2006).
10. Korup, O., Montgomery, D. R. & Hewitt, K. *Proc. Natl Acad. Sci. USA* **107,** 5317–5322 (2010).
11. Peters, S. E. *J. Geol.* **114,** 391–412 (2006).
12. Sadler, P. M. & Jerolmack, D. J. in *Strata and Time: Probing the Gaps in Our Understanding* (eds Smith, D. & Burgess, P.) (Geol. Soc. Lond. Spec. Publ., in the press).
13. Sadler, P. *Geol. Soc. Am. Abstr. Programs* **45,** 86 (2013).
14. Herman, F. *et al. Nature* **504,** 423–426 (2013).

Fly with a little flap from your friends

In-air measurements of northern bald ibises flying in a V formation show that the birds conform to predictions for saving energy by regulating their relative body position and synchronizing their flapping motion. SEE LETTER P.399

FLORIAN T. MUIJRES &
MICHAEL H. DICKINSON

The elegant V formations of migrating birds provide a picturesque harbinger of summer's end, but why do the birds fly in such a precise formation? There are rumours that Allied bomber pilots during the Second World War noticed that their fuel economy increased when their squadrons flew in a V formation. Although these apocryphal tales have not been confirmed, the energy-saving benefits of formation flying have been reported in both civil[1] and military[2] aviation. For example, by maintaining one wing tip in the wake of a forward plane, a fighter jet can reduce its energy consumption by up to 18% (ref. 2). However, exploiting the benefits of formation flight is more challenging for birds than for fixed-wing aircraft — birds not only need to adjust their position relative to each other, but also must synchronize their wingbeat patterns[3]. On page 399 of this issue, Portugal *et al.*[4] show that at least one bird species exhibits the requisite synchronization of body position and flapping motion to reduce energetic cost during migratory flight.

The principle by which formation flight saves energy derives from the way wings disturb the air as they move[1,5]. To create lift, wings accelerate airflow over their top surface compared with their bottom surface. Thus, relative to the still air through which they move, wings create a net circular flow of air that is directed rearward over the top surface and forward under the bottom surface. The greater the circulation a wing creates, the higher the lift it produces. At each wing tip, however, the circulation around the wing rolls up into a tip vortex, which extends backward like a tube,
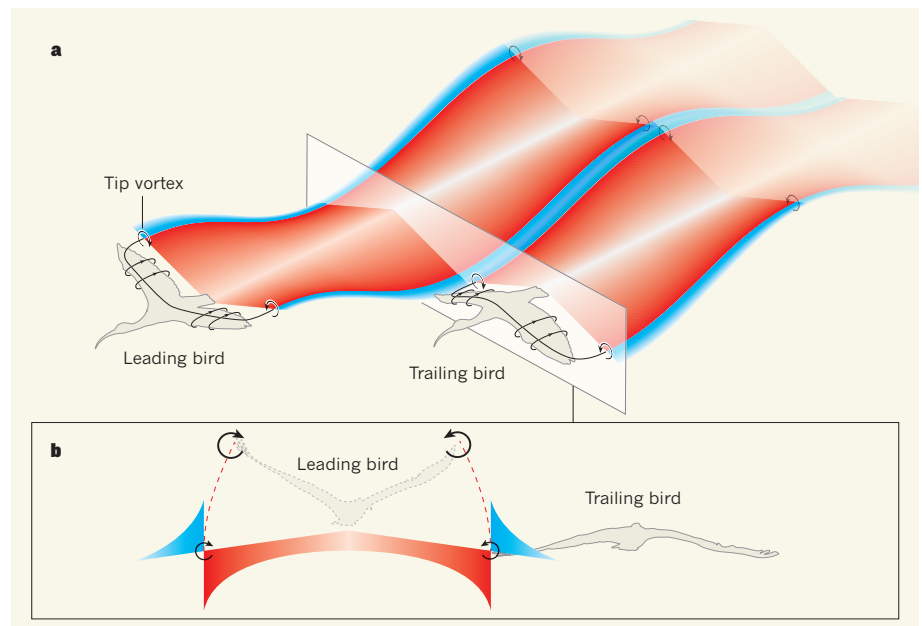

Figure 1 | Spatial synchrony. Flight creates a looping motion of air around a bird's wings; at the wing tips this circulation forms a vortex, creating air movement that extends behind the bird. Airflow down the middle of this wake is directed downwards (the downwash; red), whereas the area outside the tip vortices is a region of upwash (blue). A bird flying behind another bird experiences the aerodynamic forces of the downwash and upwash created by the leading bird (**a**, side view; **b**, rear view). Portugal and colleagues[4] show that northern bald ibises spatially synchronize their wing movements while flying in a V formation, such that the trailing bird's wing moves through the area of maximum upwash created by the leading bird. This results in more-efficient lift production and energy savings.

LETTER

A signature of transience in bedrock river incision rates over timescales of 10^4–10^7 years

Noah J. Finnegan[1], Rina Schumer[2] & Seth Finnegan[3]

Measured rates of river incision into bedrock are commonly interpreted as proxies for rates of rock uplift (see refs 1 and 2, for example) and indices of the strength of climatic forcing of erosion over time (see refs 3 and 4, for example). This approach implicitly assumes that river incision rates are in equilibrium with external forcings over a wide range of timescales. Here we directly test this assumption by examining the temporal scaling of bedrock river incision from 155 independent measurements of river incision compiled from 14 sites. Of these sites, 11 exhibit a negative power-law dependence of bedrock river incision rate on measurement interval, a relationship that is apparent over timescales of 10^4–10^7 years and is independent of tectonic and geomorphic setting. Thus, like rates of sediment accumulation[5], rates of river incision into bedrock exhibit non-steady-state behaviour even over very long measurement intervals. Non-steady-state behaviour can be explained by episodic hiatuses in river incision triggered by alluvial deposition, if such hiatuses have a heavy-tailed length distribution[6]. Regardless of its cause, the dependence of incision rate on measurement interval complicates efforts to infer tectonic or climatic forcing from changes in rates of river incision over time or from comparison of rates computed over different timescales.

Unglaciated topography is shaped by competition between tectonic uplift and bedrock river incision[7]. The potential for rivers to grow steeper, convey more water via orographic precipitation and thus become more erosive with higher rates of tectonic uplift suggests that rates of surface erosion should evolve to match rates of rock uplift in actively uplifting ranges[8]. At the same time, climate-driven changes in sediment supply and water discharge to rivers are thought to modulate rates of vertical river incision into rock over geologic time[9,10]. These arguments imply that measured rates of bedrock river incision can constrain active tectonic processes as well as temporal variability in the strength of climate forcing of erosion.

Measured rates of land-surface change in aggradational (formed by sediment deposits) settings, in contrast, exhibit a negative power-law dependence of accumulation rate on measurement interval that is not directly attributable to tectonic or climatic forcing[11]. This 'Sadler effect' arises when the duration–frequency distribution of hiatuses between intervals of accumulation has a heavy-tailed distribution[6]. Such distributions emerge from a variety of stochastic sediment accumulation models[6]. Over measurement intervals smaller than the longest hiatus, sedimentary sequences incorporate longer hiatuses at longer timescales and thus average accumulation rates tend to decline with measurement interval. It is unclear whether information about external climatic or tectonic forcing can then be recorded[6]. For example, an analysis of clastic coastal and continental shelf deposits indicates that only for measurement intervals exceeding 10^4–10^5 years do rates of sediment accumulation cease declining and therefore begin to reflect tectonic subsidence rates[5]. This measurement interval corresponds to the longest recorded hiatus.

A bedrock river is commonly conceptualized as an alluvial river bed overlying a bedrock channel bed that is incised only when the stripping of deposited alluvial material exposes bedrock to processes of abrasion,

weathering and plucking[12]. Hiatuses in incision begin when the alluvial bed aggrades and end when its elevation returns to that of the bedrock channel, for example following flood scour[12] (Fig. 1a, b). If the long time series of alluvial bed elevation can be described as a stochastic process[6,12], then the return time to bedrock will follow a power-law frequency distribution in the long time limit[6]. This is true whether aggradation and scour events follow a simple random walk process[13], a long-range correlated random process, or a random walk marked by power-law periods between deposition or erosional events[14]. Under this model, bedrock incision rate will decline with measurement interval according to a negative power-law relationship (Fig. 1c). The measurement interval over which a system exhibits negative power-law rate scaling is related to the longest physically possible hiatus duration in the period of record. Only over timescales exceeding the duration of the longest possible hiatus can changes in river incision rate be confidently interpreted in terms of tectonic or climatic forcing.

It is widely recognized that mass-wasting triggers rapid and deep alluvial bed aggradation in bedrock channels following earthquakes[15], fires[16] and large storms[17]. Additionally, both rapid scour and deposition of alluvium occurs during floods in bedrock channels. Given the stochastic nature of these processes governing alluvial bed elevation change[18], the potential exists for a negative power-law dependence of bedrock river incision rates on measurement interval. Although numerical modelling suggests that steady-state bedrock incision arises over relatively short measurement intervals (10^3 years) despite stochastic forcing of sediment supply[12], a review of bedrock incision records in the southeastern USA[19] observed a negative scaling of bedrock incision rates with measurement intervals of 10^3–10^7 years. Another study observed negative rate scaling for a variety of erosion processes over similar timescales[20]. Therefore, the fidelity of the process of bedrock river incision as a recorder of external climatic and tectonic forcing remains uncertain.

To test for a dependency of bedrock river incision rate on measurement interval, we compiled 14 bedrock river incision data sets that each span at least one order of magnitude in time (see Methods and Supplementary Table 1). To avoid the spurious correlation that arises from plotting a rate against its own denominator (measurement interval), we computed the power-law relationship between cumulative bedrock incision and measurement interval for each of the 14 data sets (see Methods). The temporal scaling of cumulative bedrock incision can then be related to the temporal scaling of bedrock incision rate by subtracting one from the cumulative incision versus measurement interval power-law exponent, herein referred to as β (Fig. 1c)[5]. Of the 14 data sets, 11 exhibit values of β that are less than one, implying a negative power-law dependence of incision rate on measurement interval (Fig. 2; Extended Data Table 1). For the entire data set, the mean power-law exponent relating cumulative river incision and measurement interval is about 0.8 (implying a rate versus measurement interval exponent of about −0.2). In addition, we find that the apparent negative power-law dependence of incision rate on measurement interval persists over four orders of magnitude in time (10^4–10^7 years) (Fig. 3). Because tectonically inactive rivers tend to preserve longer incision records than tectonically active
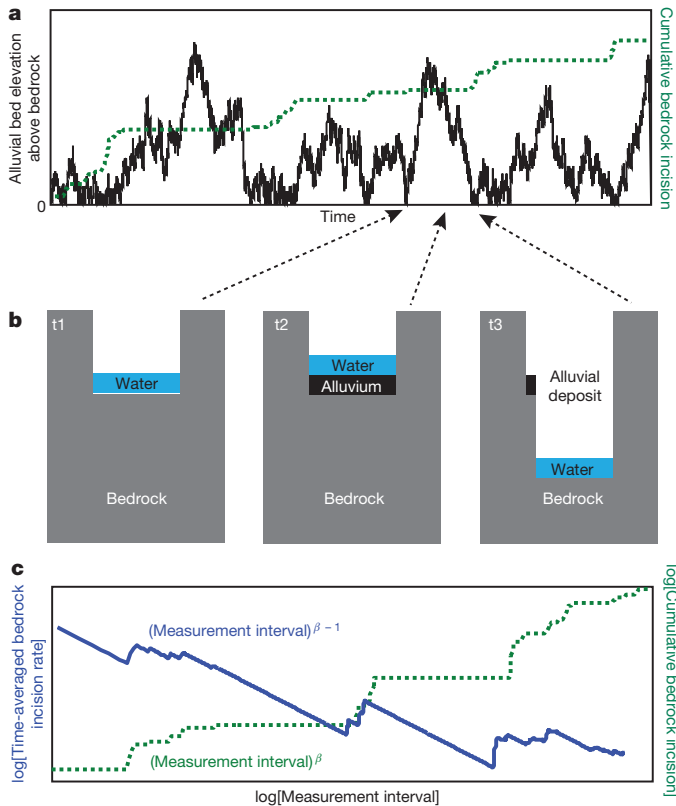
Figure 1 | The connection between stochastic alluvial bed elevation change, cumulative bedrock incision and incision rate scaling. a, Random-walk simulation of alluvial bed elevation (black line) and cumulative bedrock incision (dashed green line), assuming incision rate is constant when the bed is unburied. **b**, Bedrock canyon evolution implied by simulation. **c**, Plot of the logarithm of cumulative incision (dashed green line) and the logarithm of time-averaged incision rate (solid blue line) versus the logarithm of the measurement interval calculated from the synthetic incision record in **a**. Adjacent to each curve is the form of the power-law relationship of that variable (cumulative bedrock incision or time-averaged bedrock incision rate) to measurement interval in terms of the power-law exponent relating cumulative incision to measurement interval, β.

rivers, it is impossible to completely de-convolve measurement interval and tectonic setting. Nevertheless, we see no evidence to suggest that the observed scaling is strongly influenced by tectonic setting (Fig. 3; Extended Data Table 1). Lastly, we note that a negative power-law dependence of incision rate on measurement interval is apparent regardless of the particular landform used to constrain river incision (Extended Data Table 1). Because preservation of paired strath terraces is promoted by channel narrowing, which is a common response to accelerating incision[21], it is conceivable that the terrace record could be biased towards settings with accelerating incision and hence negative power-law rate scaling. However, a negative power-law dependence of incision rate on measurement interval is also recorded in unpaired terraces, caves and incised volcanic deposits, which should not be subject to the same preservation bias because they do not require valley narrowing for preservation. Consequently, it is unlikely that our findings simply reflect a preservation bias.

Rates of bedrock incision recorded during floods[22] and over short measurement intervals[23] are usually too large to be sustained over geologic timescales, implying that long hiatuses must separate intervals of incision. Evidence that such hiatuses have a power-law distribution in time (and are therefore probably stochastic in origin) is supported by the negative power-law dependence of incision rate on measurement interval that we observe over 10^4–10^7 years. Physical evidence for extremely long incision hiatuses in bedrock exists in the Himalayas, where valley fills can persist for over 10^5 years (ref. 24). Therefore it is possible that stochastic forcing from processes of sediment transport and delivery may be recorded in
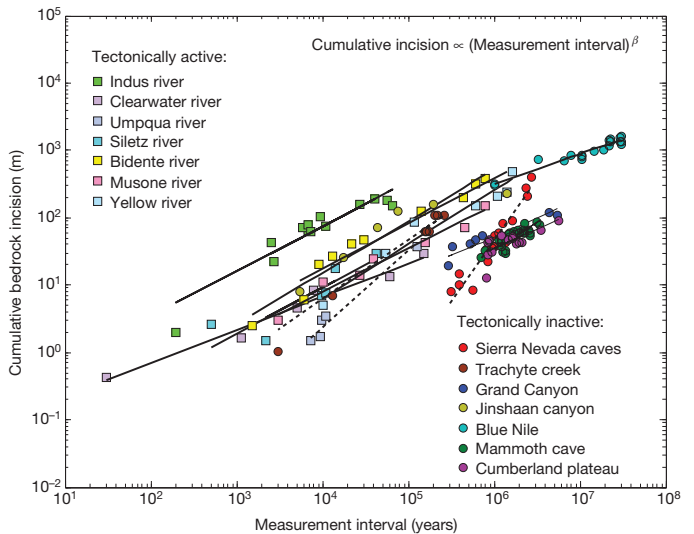

Figure 2 | Cumulative bedrock incision as a function of measurement interval. Log–log plot of cumulative incision versus measurement interval for the 14 data sets. Best-fit lines reflect the mean slopes and intercepts derived from the error analysis. Dashed lines indicate slopes (that is, β) greater than or equal to one. Solid lines indicate slopes less than one.

rates of bedrock incision even over measurement intervals exceeding 10^5 years.

It has also been argued that gravel aggradation modulated by Quaternary climate changes provides an external mechanism for generating incisional hiatuses in bedrock channels[4,10]. In this case, return time distribution theory would predict a levelling out of incision rates at the period of the forcing and thus a transition to an exponent of 1 on a plot of cumulative incision versus measurement interval. For example, in numerical experiments in which incision hiatuses are driven by glacial–interglacial climate cycles, rates of vertical incision show little change once averaged over the 10^5-year interval that corresponds to the dominant period of late Pleistocene glaciations[10]. In contrast, we find that the negative power-law dependence of incision rate on measurement interval persists over four orders of magnitude in time (10^3–10^7 years) (Fig. 3), and—importantly—over intervals much longer than the period of any known periodic climate forcing. This suggests that, globally, hiatuses in river incision into bedrock may not be coupled in a simple linear way to periodic Pleistocene climate forcing, as has been frequently suggested.

If incisional hiatus length is instead imposed by something intrinsic to the process that generates hiatuses (for example, maximum landslide
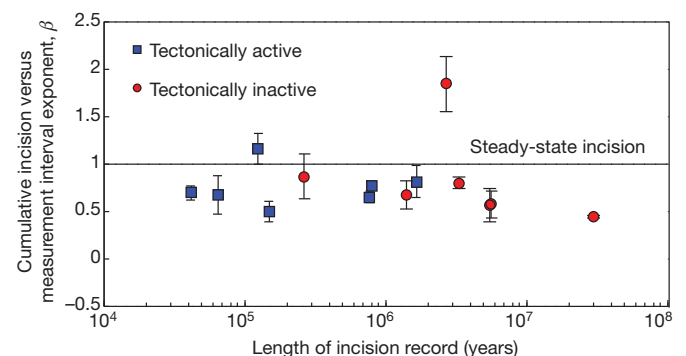

Figure 3 | Cumulative bedrock incision versus measurement interval exponent β as a function of incision record length. Data points are the mean exponent calculated from the error analysis. Error bars represent $\pm1\sigma$ derived from the error analysis. Data points plotted above the steady-state incision line reflect rates of incision that increase with measurement interval. Data points plotted below the steady-state incision line reflect rates of incision that decrease with measurement interval.

size), there is no evidence to support the existence of such a limit in the data examined here. Long-term average rates of bedrock incision are thus apparently inseparable from the interval over which they are measured. Before incision rates at different locations can be meaningfully compared, the rate-measurement interval scaling of each location must first be quantified and then the incision rates need to be normalized to a particular measurement interval. The data compiled here also suggest that comparisons between river incision rates and, for example, thermochronologic ages or geodetic rates of surface uplift may be complicated by the fact that incision rates depend on measurement interval, as well as tectonics and climate, as also argued by ref. 20. However, to the extent that stochastic variation in sediment input to channels is regionally coherent[25], the incision histories of nearby catchments might be quite similar, even if they do not record tectonic or climatic forcing in a straightforward way.

Our inference that the dependence of incision rate on measurement interval reflects the influence of episodic alluvial aggradation is supported by the observation that bedrock river channels are usually covered in debris, even in tectonically active settings[12,26,27]. The incision scaling observed on the Blue Nile river[28], if it arises from power-law hiatuses, implies an instantaneous incision of about 0.7 m in 1 year, but only 116 m after 10^5 years. Thus, only during 0.2% of a 10^5-year-long record (that is, 166 years) would any channel incision occur. In other words, as observers, we are far more likely to encounter a channel in a state of non-incision. This suggests that an understanding of the processes that generate incisional hiatuses is arguably more important to understanding rates of landscape change than is an understanding of the incision process itself, as has also been argued by ref. 12. Our analysis also suggests that apparent recent increases in river incision rates should be an expected consequence of measuring bedrock river incision rates over measurement intervals that do not incorporate long hiatuses, as argued by ref. 10.

Do the same issues that complicate the interpretation of river incision rates also affect landscape-scale erosion rates? A study of sediment yields in steep, mountainous catchments on decadal measurement intervals suggests that landscape-scale erosion rates (as opposed to fluvial incision rates) are biased towards slow rates over short measurement intervals because of infrequently sampled catastrophic erosion events[25]. This scaling is the opposite of what we observe in the case of river incision, where shorter measurement intervals tend to yield higher rate estimates. One potential explanation for this apparent contradiction is that materials eroded from hill slopes are subsequently deposited in channels, where they may cause hiatuses in bedrock channel incision. Infrequent, large hill-slope erosion events could therefore trigger infrequent but long-duration hiatuses in bedrock channel incision. That said, in general landscape-scale erosion rates show little apparent dependence on measurement interval[29], an observation that has been attributed to the averaging out of local stochasticity with increasing spatial scale of measurement[29]. Thus, the influence of locally stochastic erosional processes on temporal rate scaling may depend both on the specific process in question and on the spatial scale examined.

METHODS SUMMARY

We compiled 14 bedrock river incision data sets that span at least one order of magnitude in time (Supplementary Table 1), encompassing a total of 155 measurements of river incision. We define tectonically active settings as those regions with documented tectonically driven rock uplift. Each of the tectonically active data sets was also taken from a paper (see the Extended Methods for citations) that measured river incision to constrain active tectonic processes. Tectonically inactive settings did not meet these criteria. We use reported or estimated uncertainties for each measurement of cumulative bedrock incision and measurement interval to define the uncertainty for each data point in each data set. We performed a Monte Carlo error analysis for each data set in which we calculated 3,000 linear fits between the logarithm of cumulative bedrock incision and the logarithm of measurement interval. Measurement interval for a cumulative river incision measurement is equivalent to the age of the landform used to constrain incision. This is because cumulative river incision for all data points is computed between the modern channel elevation and

the palaeo-channel elevation. We do not calculate incision between dated landforms because such estimates do not represent statistically independent measurements of incision. For each model iteration, we assigned incision and age errors by selecting randomly from a normal error distribution for each data point with a standard deviation corresponding to the reported or estimated uncertainty in landform age and elevation. Slope and intercept distributions were created for each data set from the results of the Monte Carlo simulation to define power-law exponents relating cumulative incision and measurement interval, as well as corresponding uncertainties. Because our explanatory variable (measurement interval) has significant uncertainty, we use a total-least-squares regression method to quantify slope.

Online Content Any additional Methods, Extended Data display items and Source Data are available in the online version of the paper; references unique to these sections appear only in the online paper.

1. Pazzaglia, F. J. & Brandon, M. T. A fluvial record of long-term steady-state uplift and erosion across the Cascadia forearc high, western Washington State. *Am. J. Sci.* **301,** 385–431 (2001).
2. Burbank, D. W. *et al.* Bedrock incision, rock uplift and threshold hillslopes in the northwestern Himalayas. *Nature* **379,** 505–510 (1996).
3. Leland, J., Reid, M. R., Burbank, D. W., Finkel, R. & Caffee, M. Incision and differential bedrock uplift along the Indus River near Nanga Parbat, Pakistan Himalaya, from ^{10}Be and ^{26}Al exposure age dating of bedrock straths. *Earth Planet. Sci. Lett.* **154,** 93–107 (1998).
4. Bull, W. L. & Knuepfer, P. L. K. Adjustments by the Charwell River, New Zealand, to uplift and climatic changes. *Geomorphology* **1,** 15–32 (1987).
5. Jerolmack, D. J. & Sadler, P. Transience and persistence in the depositional record of continental margins. *J. Geophys. Res.* **112,** F03S13 (2007).
6. Schumer, R. & Jerolmack, D. J. Real and apparent changes in sediment deposition rates through time. *J. Geophys. Res.* **114,** F00A06 (2009).
7. Howard, A. D., Dietrich, W. E. & Seidl, M. A. Modeling fluvial erosion on regional to continental scales. *J. Geophys. Res.* **99,** 13971–13986 (1994).
8. Whipple, K. X. Bedrock rivers and the geomorphology of active orogens. *Annu. Rev. Earth Planet. Sci.* **32,** 151–185 (2004).
9. Molnar, P. *et al.* Quaternary climate change and the formation of river terraces across growing anticlines on the north flank of the Tien Shan, China. *J. Geol.* **102,** 583–602 (1994).
10. Hancock, G. S. & Anderson, R. S. Numerical modeling of fluvial strath-terrace formation in response to oscillating climate. *Geol. Soc. Am. Bull.* **114,** 1131–1142 (2002).
11. Sadler, P. M. Sediment accumulation rates and the completeness of stratigraphic sections. *J. Geol.* **89,** 569–584 (1981).
12. Lague, D. Reduction of long-term bedrock incision efficiency by short-term alluvial cover intermittency. *J. Geophys. Res.* **115,** F02011 (2010).
13. Redner, S. *A Guide to First-Passage Processes* Chs 1 and 3 (Cambridge Univ. Press, 2007).
14. Ding, M. Z. & Yang, W. M. Distribution of the first return time in fractional Brownian-motion and its application to the study of on-off intermittency. *Phys. Rev. E* **52,** 207–213 (1995).
15. Yanites, B. J., Tucker, G. E., Mueller, K. J. & Chen, Y.-G. How rivers react to large earthquakes: evidence from central Taiwan. *Geology* **38,** 639–642 (2010).
16. Roering, J. J. & Gerber, M. Fire and the evolution of steep, soil-mantled landscapes. *Geology* **33,** 349–352 (2005).
17. Benda, L. The influence of debris flows on channels and valley floors in the Oregon Coast Range, U.S.A. *Earth Surf. Process. Landf.* **15,** 457–466 (1990).
18. Jerolmack, D. J. & Paola, C. Shredding of environmental signals by sediment transport. *Geophys. Res. Lett.* **37,** L19401 (2010).
19. Mills, H. H. Apparent increasing rates of stream incision in the eastern United States during the late Cenozoic. *Geology* **28,** 955–957 (2000).
20. Gardner, T. W., Jorgensen, D. W., Shuman, C. & Lemieux, C. R. Geomorphic and tectonic process rates: effects of measured time interval. *Geology* **15,** 259–261 (1987).
21. Whittaker, A. C., Cowie, P. A., Attal, M., Tucker, G. E. & Roberts, G. P. Bedrock channel adjustment to tectonic forcing: implications for predicting river incision rates. *Geology* **35,** 103–106 (2007).
22. Lamb, M. P. & Fonstad, M. A. Rapid formation of a modern bedrock canyon by a single flood event. *Nature Geosci.* **3,** 477–481 (2010).
23. Schaller, M. *et al.* Fluvial bedrock incision in the active mountain belt of Taiwan from in situ-produced cosmogenic nuclides. *Earth Surf. Process. Landf.* **30,** 955–971 (2005).
24. Blöthe, J. H. & Korup, O. Millennial lag times in the Himalayan sediment routing system. *Earth Planet. Sci. Lett.* **382,** 38–46 (2013).
25. Kirchner, J. W. *et al.* Mountain erosion over 10 yr, 10 k.y., and 10 m.y. time scales. *Geology* **29,** 591–594 (2001).
26. Turowski, J. M., Hovius, N., Wilson, A. & Horng, M.-J. Hydraulic geometry, river sediment and the definition of bedrock channels. *Geomorphology* **99,** 26–38 (2008).
27. Ouimet, W. B., Whipple, K. X., Royden, L. H., Sun, Z. & Chen, Z. The influence of large landslides on river incision in a transient landscape: eastern margin of the Tibetan Plateau (Sichuan, China). *Geol. Soc. Am. Bull.* **119,** 1462–1476 (2007).
28. Gani, N. D. S., Gani, M. R. & Abdelsalam, M. G. Blue Nile incision on the Ethiopian Plateau: pulsed plateau growth, Pliocene uplift, and hominin evolution. *GSA Today* **17** (9), 4–11 (2007).

29. Sadler, P. & Jerolmack, D. J. Scaling laws for aggradation, denudation and progradation rates: the case for time-scale invariance at sediment sources and sinks. In *Strata and Time: Probing the Gaps in Our Understanding* (eds Smith, D. & Burgess, P.) (Geological Society of London Special Publication, in the press).

METHODS

To test for a dependence of river incision rate on measurement interval, we compiled 14 bedrock river incision data sets, each of which spans at least one order of magnitude in time (Supplementary Table 1), encompassing a total of 155 independent measurements of river incision. First we describe the incision data sources. Then, we describe the statistical analyses performed on the data to constrain the relationship between cumulative bedrock incision and measurement interval for the 14 data sets.

We provide the location and citation for each of the 14 incision data sets used in the analysis. In addition, we describe how both landform ages and uncertainties and cumulative bedrock incision values and uncertainties were determined for each data set. Of the 14 data sets, we identified tectonically active settings as those regions with documented tectonically driven rock uplift. In addition, each of the tectonically active data sets was taken from a paper that measured river incision to constrain active tectonic processes. Areas identified as tectonically inactive did not meet these criteria.

Middle Gorge of the Indus river, Pakistan. We used the weighted average ages and corresponding uncertainties and elevations reported in table 2 of ref. 3. Elevation uncertainty was assigned according to section 3.1 of ref. 3. We ignored point 5 in table 2 of ref. 3, following the interpretation of the authors.

Clearwater river, Olympic Mountains, Washington (state), USA. We used the ages and age ranges from figure 4 of ref. 30 to define the ages and age uncertainties for terraces. We digitized the terrace elevations from figure 4 of ref. 30 and used the reported elevation uncertainties in table 1 of ref. 30.

Umpqua and Siletz rivers, Oregon Coast Range, Oregon, USA. We used the ages and elevations along with their corresponding uncertainties as reported in table 1 of ref. 31. We selected only the Siletz and Umpqua River data sets as these span the longest period of time.

Bidente and Musone rivers, Northern Apennines, Italy. We used the ages and elevations along with their corresponding uncertainties as reported in tables 2 and 4 of ref. 32.

Yellow river, Linxia basin, eastern Tibetan plateau margin, China. We used the ages and bedrock elevations reported in table 1 of ref. 33. We assume a 10% uncertainty for age and a 5 m uncertainty in elevation, in keeping with the largest observed uncertainties in other data sets.

Sierra Nevada caves, California, USA. We used the ages and elevations along with their corresponding uncertainties as reported in table 2 of ref. 34.

Trachyte creek, Colorado plateau, Arizona, USA. We used strath ages and corresponding uncertainties reported in table 3 of ref. 35. Strath elevations were obtained from table 4 of ref. 35. We assigned an uncertainty in elevation of 5 m.

Grand Canyon, Colorado river, Colorado plateau, Arizona, USA. To avoid comparing reaches with different rates of tectonic forcing, we selected only data identified by the authors of ref. 36 as part of the "Western [Fault] Block" of the Grand Canyon because it is the longest record presented. Ages and uncertainties as well as strath elevations were obtained from table 2 of ref. 36. Strath elevation uncertainties were estimated to be half of the maximum pool depth reported in table 2 of ref. 36.

Yellow river, Jinshaan canyon, Oordos plateau, China. Strath ages and uncertainties were obtained from table 1 of ref. 37. Terrace elevations were selected from the Qilangwo locale in table 2 of ref. 37. Uncertainties in elevation were assumed to be 5 m.

Grand Canyon of the Nile, Blue Nile river, Ethiopia[28]. Ages and elevations were digitized from figure 5 of ref. 28. Uncertainties of 10% were assumed for age, and 5 m uncertainties were assigned to elevations.

Mammoth cave, Green river, Kentucky, USA. Ages and uncertainties were obtained from table 2 of ref. 38. Elevations were obtained from table 3 of ref. 38. Uncertainties in elevation were assigned according to the Methods of ref. 38.

Cumberland river, Cumberland plateau, Kentucky and Tennessee, USA. Ages and uncertainties as well as elevations were obtained from table 1 of ref. 39. Uncertainties in elevation were assigned to be 2 m, because of the similarity of this study to ref. 38.

We performed a Monte Carlo error analysis for each data set, in which we calculated 3,000 linear fits between the logarithm of cumulative bedrock incision and the logarithm of measurement interval. The measurement interval for a river incision measurement is equivalent to the age of the landform used to constrain incision. This is because cumulative river incision for all data points is computed between the modern channel and the palaeo-channel. We do not calculate incision between dated landforms because such estimates do not represent statistically independent measurements of incision. For each model iteration, we assigned incision and age errors by selecting randomly from a normal error distribution for each data point with a standard deviation corresponding to the reported or estimated uncertainty in landform age and elevation. Slope and intercept distributions were created for each data set from the results of the Monte Carlo simulation to define power-law exponents relating cumulative incision and measurement interval, as well as corresponding uncertainties. Because our explanatory variable (measurement interval) has significant uncertainty, we use a total-least-squares regression method to quantify slope.

30. Wegmann, K. W. & Pazzaglia, F. J. Holocene strath terraces, climate change, and active tectonics: the Clearwater River basin, Olympic Peninsula, Washington State. *Geol. Soc. Am. Bull.* **114,** 731–744 (2002).
31. Personius, S. F. Late Quaternary stream incision and uplift in the forearc of the Cascadia subduction zone, western Oregon. *J. Geophys. Res.* **100,** 20193–120210 (1995).
32. Wegmann, K. W. & Pazzaglia, F. J. Late Quaternary fluvial terraces of the Romagna and Marche Apennines, Italy: climatic, lithologic, and tectonic controls on terrace genesis in an active orogen. *Quat. Sci. Rev.* **28,** 137–165 (2009).
33. Li, J.-J. *et al.* Magnetostratigraphic dating of river terraces: rapid and intermittent incision by the Yellow River of the northeastern margin of the Tibetan Plateau during the Quaternary. *J. Geophys. Res.* **102,** 10121–10132 (1997).
34. Stock, G. M., Anderson, R. S. & Finkel, R. C. Rates of erosion and topographic evolution of the Sierra Nevada, California, inferred from cosmogenic ^{26}Al and ^{10}Be concentrations. *Earth Surf. Process. Landf.* **30,** 985–1006 (2005).
35. Cook, K. L., Whipple, K. X., Heimsath, A. M. & Hanks, T. C. Rapid incision of the Colorado River in Glen Canyon — insights from channel profiles, local incision rates, and modeling of lithologic controls. *Earth Surf. Process. Landf.* **34,** 994–1010 (2009).
36. Karlstrom, K. E. *et al.* ^{40}Ar/^{39}Ar and field studies of Quaternary basalts in Grand Canyon and model for carving Grand Canyon: quantifying the interaction of river incision and normal faulting across the western edge of the Colorado Plateau. *Geol. Soc. Am. Bull.* **119,** 1283–1312 (2007).
37. Cheng, S., Deng, Q., Zhou, S. & Yang, G. Strath terraces of Jinshaan Canyon, Yellow River, and Quaternary tectonic movements of the Ordos Plateau, North China. *Terra Nova* **14,** 215–224 (2002).
38. Granger, D. E., Fabel, D. & Palmer, A. N. Pliocene–Pleistocene incision of the Green River, Kentucky, determined from radioactive decay of cosmogenic ^{26}Al and ^{10}Be in Mammoth Cave sediments. *Geol. Soc. Am. Bull.* **113,** 825–836 (2001).
39. Anthony, D. M. & Granger, D. E. A late Tertiary origin for multilevel caves along the western escarpment of the Cumberland Plateau, Tennessee and Kentucky, established by cosmogenic ^{26}Al and ^{10}Be. *J. Caves Karst Stud.* **66,** 46–55 (2004).

Extended Data Table 1 | Power-law fits, tectonic setting and landform type for each data set

Location	Reference	Cumulative incision versus measurement interval exponent (β)	+/- 1σ	Length of incision record (kyr)	Tectonic setting	Landform
Middle gorge of the Indus river, Pakistan	3	0.67	0.19	65	Active	Unpaired strath terraces
Clearwater river, Olympic Mountains, Washington (state), USA	30	0.49	0.12	150	Active	Paired and unpaired strath terraces
Umpqua river, Oregon Coast Range, Oregon, USA	31	1.16	0.27	125	Active	Unpaired strath terraces
Siletz river, Oregon Coast Range, Oregon, USA	31	0.69	0.07	42	Active	Unpaired strath terraces
Bidente river, Northern Apennines, Italy	32	0.76	0.04	800	Active	Paired and unpaired strath terraces
Musone river, Northern Apennines, Italy	32	0.65	0.07	775	Active	Paired and unpaired strath terraces
Yellow river, Linxia Basin, eastern Tibetan plateau margin, China	33	0.8	0.16	1,660	Active	Strath terrace
Sierra Nevada caves, California, USA	34	1.84	0.28	2,700	Inactive	Cave
Trachyte creek, Colorado plateau, Arizona, USA	35	0.88	0.24	267	Inactive	Paired and unpaired strath terraces
Grand Canyon, Colorado river, Colorado plateau, Arizona, USA	36	0.57	0.17	5,500	Inactive	Miscellaneous
Yellow river, Jinshaan canyon, Oordos plateau, China	37	0.67	0.15	1,410	Inactive	Strath terrace
Gorge of the Nile, Blue Nile river, Ethiopia	28	0.44	0.01	3,002	Inactive	Dated volcanic rocks
Mammoth cave, Green river, Kentucky, USA	38	0.79	0.06	3,360	Inactive	Cave
Cumberland river, Cumberland plateau, Kentucky and Tennessee, USA	39	0.57	0.15	5,680	Inactive	Cave